

Dramatic efficacy of vemurafenib in both multisystemic and refractory Erdheim-Chester disease and Langerhans cell histiocytosis harboring the *BRAF* V600E mutation

*Julien Haroche,^{1,2} *Fleur Cohen-Aubart,^{1,2} *Jean-François Emile,³ *Laurent Arnaud,^{1,2} Philippe Maksud,⁴ Frédéric Charlotte,⁵ Philippe Cluzel,⁶ Aurélie Drier,⁷ Baptiste Hervier,^{1,2} Neïla Benameur,⁸ Sophie Besnard,⁹ Jean Donadieu,¹⁰ and Zahir Amoura^{1,2}

¹Department of Internal Medicine and French reference Center for Rare Auto-immune and Systemic Diseases, Assistance Publique-Hôpitaux de Paris (AP-HP), Pitié-Salpêtrière Hospital, Paris, France; ²Université Pierre et Marie Curie, UPMC University Paris 6, Paris, France; ³Research Unit (EA) EA4340 and Pathology Laboratory, Versailles University and AP-HP, Boulogne, France; Departments of ⁴Nuclear Medicine, ⁵Pathology, ⁶Radiology, ⁷Neuroradiology, and ⁸Pharmacy, Hôpital Pitié-Salpêtrière, University Paris 6, AP-HP, Paris, France, ⁹Department of Internal Medicine, Pontchaillou University Hospital, Rennes Cedex, France, and ¹⁰Department of Pediatrics, AP-HP, Centre de Référence des Histiocytoses, Hôpital Trousseau, Paris, France

Key Points

- Treatment with vemurafenib induced a dramatic response in 3 patients with histiocytosis harboring *BRAF* V600E mutations.
- Tumor response was observed in both Erdheim-Chester disease and Langerhans cell histiocytosis.

Histiocytoses are rare disorders of unknown origin with highly heterogeneous prognosis. *BRAF*^{V600E} gain-of-function mutations have been observed in 57% of cases of Langerhans cell histiocytosis (LCH) and 54% of cases of Erdheim-Chester disease (ECD), but not in other types of histiocytoses. Targeted therapy with an inhibitor of mutated *BRAF* (vemurafenib) improves survival of patients with melanoma. Here, we report vemurafenib treatment of 3 patients with multisystemic and refractory ECD carrying the *BRAF*^{V600E} mutation; 2 also had skin or lymph node LCH involvement. The patients were assessed clinically, biologically (CRP values), histologically (skin biopsy), and morphologically (positron emission tomography [PET], computed tomography and magnetic resonance imaging). For all patients, vemurafenib treatment led to substantial and rapid clinical and biologic improvement, and the tumor response was confirmed by PET, computed tomography, and/or magnetic resonance imaging 1 month after treatment initiation. For the first patient treated, the PET response increased between

months 1 and 4 of treatment. The treatment remained effective after 4 months of follow-up although persistent disease activity was still observed. Treatment with vemurafenib, a newly approved *BRAF* inhibitor, should be considered for patients with severe and refractory *BRAF*^{V600E} histiocytoses, particularly when the disease is life-threatening. (*Blood*. 2013;121(9):1495-1500)

Introduction

Erdheim-Chester disease (ECD) is a rare non-Langerhans cell histiocytosis, characterized by the infiltration of tissues by foamy CD68⁺ CD1a⁻ histiocytes.¹ It is a systemic disease with diverse manifestations: the clinical course mainly depends on the extent and distribution of the disease, and ranges from asymptomatic bone lesions to life-threatening manifestations.² Rare cases of ECD associated with Langerhans cell histiocytosis (LCH) have been reported.³

Unlike ECD, LCH histiocytes are CD1a⁺ and frequently infiltrate the epidermis in skin lesions.⁴ Interferon α (IFN) is generally the first choice for ECD therapy and improves survival. It should be prescribed at high dose if there is central nervous system and/or cardiovascular involvement.² However, long-term IFN treatment can lead to severe side effects and some patients are refractory to treatment. Moreover some patients with CNS and/or cardiovascular infiltrations develop secondary resistance to high-dose of IFN. Alternative treatments include recombinant human interleukin-1 receptor antagonist, cladribine, thymosine kinase inhibitors, autologous hematopoietic stem cell transplantation.² However, the optimal second line therapeutic strategy remains to be defined, mostly because these

treatments have been evaluated in only small numbers of patients. Despite recent therapeutic progress the overall mortality remains high (18% of the 84 ECD patients seen at our institution). *BRAF*^{V600E} mutations have been observed in 38% to 69% of cases of LCH.⁵⁻⁷ We recently reported *BRAF*^{V600E} mutations in 54% of 24 patients with ECD.⁸ Vemurafenib, an inhibitor of mutant *BRAF*, has shown some efficacy against 2 diseases (melanoma and hairy-cell leukemia) associated with the *BRAF*^{V600E} mutation.^{9,10}

Methods

This study was approved by the ethics committee Ile de France III (#2011-A00447-34) and conducted in accordance with the Declaration of Helsinki.

Patient no. 1

A 65-year-old man presented in October 2010 with elevated serum creatinine and C-reactive protein (CRP) levels found on routine blood testing. Abdominal computed tomography (CT) disclosed retroperitoneal

Submitted July 27, 2012; accepted November 18, 2012. Prepublished online as Blood First Edition paper, December 20, 2012; DOI: 10.1182/blood-2012-07-446286.

*J.H., F.C.-A., J.-F.E., and L.A. contributed equally to this work
There is an Inside *Blood* commentary on this article in this issue.

The publication costs of this article were defrayed in part by page charge payment. Therefore, and solely to indicate this fact, this article is hereby marked "advertisement" in accordance with 18 USC section 1734.

© 2013 by The American Society of Hematology

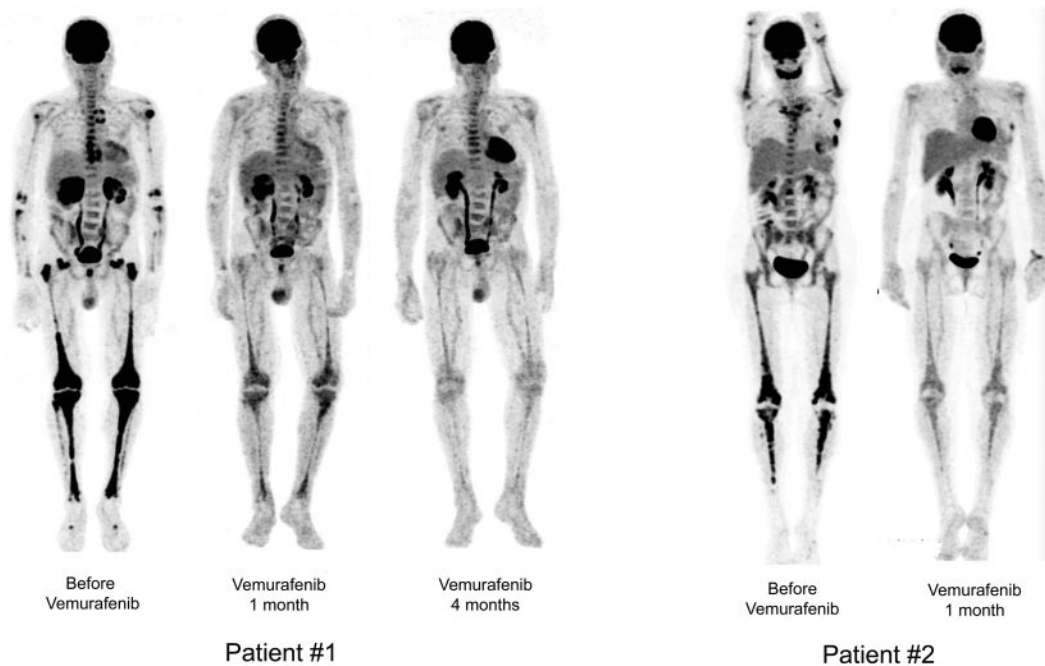


Figure 1. Sequential PET. Patient no. 1 (left): Sequential PET showing high initial pathologic uptake of ^{18}F -fluorodeoxyglucose in soft tissue and bones before vemurafenib treatment, and significantly less uptake after 1 month and major regression after 4 months of vemurafenib treatment. Patient no. 2 (right): Similar substantial reduction of ^{18}F -fluorodeoxyglucose uptake in all tissues involved. Reconstruction algorithm: OSEM_3D (5 iterations, 16 subsets, 9 mm Gauss filter). Volume rendering: Maximum Intensity Projection (Osirix Software). Display: BW inverse logarithmic table and range (min value = 0, max = 2.7 for SUV).

fibrosis complicated by bilateral hydronephrosis with sheathing of the abdominal aorta. Double ureteral pigtail stents were inserted and because hydronephrosis relapsed, bilateral nephrostomy was performed. Long-bone X-rays showed typical bilateral and symmetric cortical osteosclerosis in the lower limbs. A biopsy sample of the perirenal fibrosis showed numerous foamy CD68^+ CD1a^- histiocytes. A diagnosis of ECD was established. Cerebral magnetic resonance imaging (MRI) showed sinus osteosclerosis; on cardiac MRI, the pericardium appeared thickened and there was specific infiltration of the auriculo-ventricular sulcus. Positron emission tomography (PET) revealed an intense uptake in the lower limbs and in the thoracic aorta.

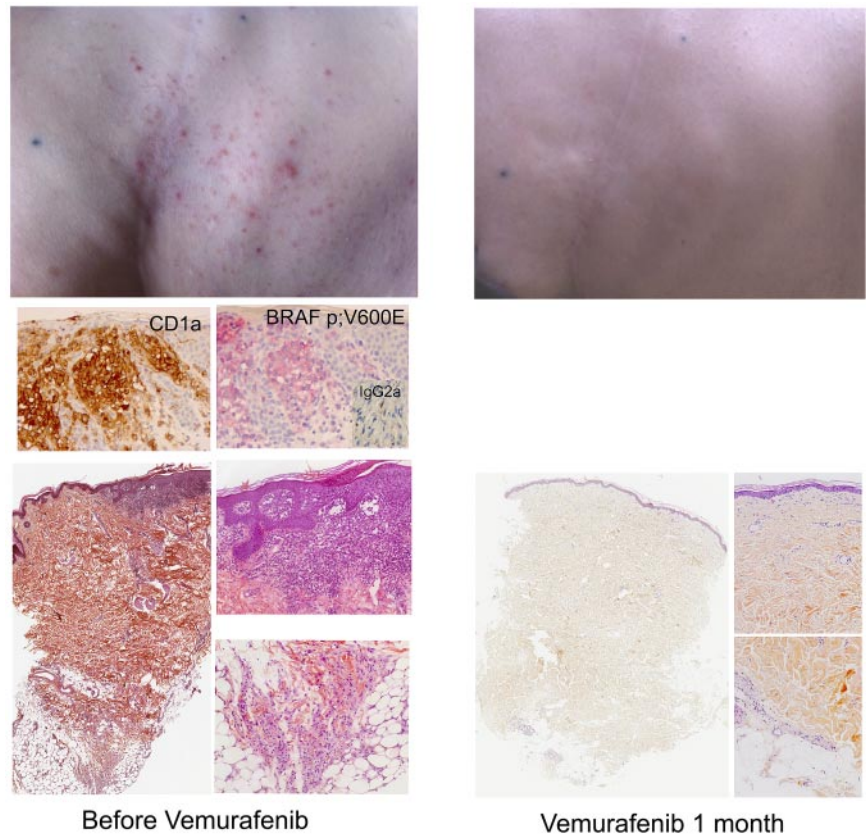
Pegylated interferon α (PEG-IFN) treatment was started in July 2011, at 135 $\mu\text{g}/\text{w}$ for 4 weeks, and was then increased to 180 $\mu\text{g}/\text{w}$ due to cardiac involvement. Double ureteral pigtail stents were implanted to replace the nephrostomy and the blood creatinine concentration remained stable at 115 μM . In January 2012, the CRP level was 21 mg/L, and the creatinine level was 137 μM . The patient developed pruritus, and gamma-glutamyl transferase (GGT) activity was 936 U/L (normal 12-55) and alkaline phosphatase activity was 644 U/L (normal 40-120). Abdominal CT showed the persistence of sheathing of the whole aorta. Bilateral hydronephrosis had increased and there was a left renal artery stenosis. Liver MRI and biopsy showed no or only minor abnormalities, and in particular no histiocytes or signs of sclerosing cholangitis. PET revealed that the number of lesions and uptake by the lesion had increased, that is, hypermetabolism of the long bones of the lower limbs, and of thoracic and abdominal aorta, mediastinum and retroperitoneum (Figure 1). Cardiac MRI findings were unchanged. Angioplasty of the left renal artery with stent implantation was performed. In February 2012, the IFN dose was increased (to 180 $\mu\text{g}/\text{w}$ PEG-IFN alternating with 270 $\mu\text{g}/\text{w}$) due to the absence of response to treatment; this was followed by depression and fatigue. The depressive symptoms persisted despite administration of antidepressant drugs, leading to the IFN treatment being stopped in March 2012. The creatinine level increased to 190 μM , and consequently the double ureteral pigtail stents were replaced by thermoformable spiral metallic stents.

Patient no. 2

A 59-year-old woman was referred to us in February 2011 with a 2-year history of bone pain in the lower limbs. For the previous 6 months she had had diabetes insipidus, right orbital pain requiring morphine, and headaches. She had a history of bilateral breast cancer in 1998 treated by right mastectomy, radiotherapy, and chemotherapy. Thoracic and abdominal CT showed peri-aortitis (involving the arch, origin of the supra-aortic vessels, and the sub-renal aorta), nodular infiltration of the epiploon, and soft-tissue thickening of the pre- and retro-sternal spaces. Cardiac MRI showed a right pseudo-tumoral atrial infiltration. Orbital MRI found a right retro-orbital infiltration and compression of the optic nerve with intense enhancement after gadolinium administration. Bone scintigraphy was highly suggestive of ECD with intense uptake in the lower limbs. A monoclonal IgA κ component (12 g/L) was found, so a bone marrow biopsy was collected and revealed 30% plasma cell infiltration; renal function and calcemia were normal, hemoglobin was 12.5 g/dL, there was no proteinuria, and no lytic bone lesions were found. Stage I myeloma in the Durie-Salmon classification was diagnosed. Celioscopy in January 2011 found a peritoneal infiltration with foamy CD68^+ CD1a^- histiocytes consistent with a diagnosis of ECD. At initial presentation, the patient had papulo-maculous squamous intertrigo-like lesions under the left breast: biopsies showed Langerhans cell infiltrate in the epidermis and non-Langerhans cell infiltrate in the hypodermis (Figure 2). Initial PET revealed intense uptake in the retro-orbital space, right atrium, and abdominal aorta, and bilateral and symmetric uptake in the diaphyseal and metaphyseal regions of the long bones (Figure 1) typical of ECD. These findings led to a diagnosis of ECD associated with histologic lesions of LCH in the skin. The most severe symptoms, requiring therapy, were due to ECD (peri-aortitis, bone pain, pseudo-tumoral atrial infiltration, mesenteric localization, and right retro-orbital involvement). The associated IgA κ stage I myeloma only required monitoring.

Therapy with 135 $\mu\text{g}/\text{w}$ PEG-IFN was initiated in March 2011. Partial improvement was observed, but pain in the right eye and cardiac abnormalities persisted. The PEG-IFN dose was increased to 180 $\mu\text{g}/\text{w}$ in June 2011. In December 2011, the orbital pain had worsened and orbit MRI detected a

Figure 2. Skin lesions. LCH skin lesions in patient no. 2 disappeared after a few days of treatment with vemurafenib. Skin biopsy before treatment showing typical LCH infiltration of the epidermis and papillary dermis with CD1a⁺ histiocytes; the hypodermis is infiltrated by foamy CD68⁺CD1a⁻ histiocytes (as in the peritoneal biopsy). Immunohistochemistry confirmed the expression of BRAF by histiocytes.



new hypersignal in the right optic nerve; PET revealed intense uptake in the long bones. PEG-IFN, which had been maintained at 180 $\mu\text{g}/\text{w}$, was stopped at the beginning of March 2012 due to depression, fatigue, neutropenia ($\approx 500/\text{mm}^3$), thrombocytopenia ($46,000/\text{mm}^3$), and inefficacy against the retro-orbital involvement. The patient was re-assessed on March 23: she had fever, CRP was 89 mg/L, and PET confirmed the worsening of the retro-orbital, bone, and mediastinal involvements. Orbit MRI also showed persistence of the retro-orbital lesion (Figure 3). Treatment with 100 mg/d anakinra was initiated on March 24 and effectively reduced the fever but not the CRP value (Figure 4). Concomitantly, the cutaneous lesions relapsed leading to anakinra discontinuation on April 17. The right retro-orbital pain worsened. Skin lesions were re-biopsied and the findings were unchanged (co-existence of LCH in the epidermis and ECD in the hypodermis).

Patient no. 3

A 31-year-old woman originating from Laos was referred to our department in April 2010 for subacute renal failure, diabetes insipidus, and elevated CRP level. Physical examination identified bilateral superior and inferior eyelid xanthelasma. Blood tests confirmed elevated creatinine and CRP levels (178 μM and 147 mg/L, respectively). Abdominal CT-scan revealed retroperitoneal fibrosis and lymphadenopathy, and cerebral MRI showed that the pituitary axis was enlarged. Long bone ^{99}Tc scintigraphy showed intense metaphyseodiaphyseal uptake in femurs and tibiae. Similar hypermetabolism in the long bones and also in the spleen, and retroperitoneal adenopathies were found on PET.

Biopsy of the palpebral xanthelasma confirmed the ECD localization with foamy histiocytes. Immunohistology was positive for CD68 and negative for PS100 with a few CD1a-positive cells. Biopsies of T4 vertebra and right inferior metaphyseal femur showed the same ECD patterns, and a biopsy of a retroperitoneal node displayed characteristics of LCH with strongly positive CD1a and PS100 staining.

In April 2010, treatment with PEG-IFN (135 $\mu\text{g}/\text{w}$) was started and double ureteral pigtail stents were inserted. Ten months later, in February

2011, the CRP level was 24 mg/L, creatinine had decreased to 138 μM , and PET showed an improvement of long-bone uptake. In February 2012, the clinical status had deteriorated with new lower-limb pain and increased size of xanthelasmas. Abdominal CT scan showed enlargement of periaortic and periureteral infiltrations. Cardiac MRI, which had been normal on previous assessments, displayed a typical infiltration of the right atrial wall, atrioventricular groove, and gadolinium enhancement of the left ventricular wall, septum, and apex. The CRP level was 20 mg/L and PET disclosed a strong, new uptake in the basilar skull region. The PEG-IFN dose was increased to 180 $\mu\text{g}/\text{w}$ on March 20, but was clinically ineffective: the CRP level increased to 42 mg/L. Treatment was stopped on May 9.

Histology and molecular analyses

All biopsies (perirenal, peritoneal, skin, and bone) obtained from the 3 patients before or after vemurafenib treatment were reviewed by 2 pathologists with specialist training in histiocytosis (F.C.-A., J.-F.E.). All patients provided consent for vemurafenib treatment after the provision of counseling. Each sample was processed for immunohistochemistry with antibodies against CD1a (Beckman-Coulter), CD68 (Dako), CD163 (ThermoFisher) and S100 protein (Dako), and with VE1 (a mouse monoclonal antibody specific for the *BRAF*^{V600E} mutant, kindly provided by Prof A. von Deimling, Heidelberg University, Heidelberg, Germany). Clone L26 (anti-CD20) was used as IgG2a isotype matched control for the VE1 antibody.¹¹

BRAF^{V600E} mutations were detected as previously described.¹² DNA was extracted from formalin-fixed and paraffin-embedded (FFPE) tissues after histologic detection of histiocyte-rich areas, and pyrosequencing with PyroMark Q24 (QIAGEN) was used to detect *BRAF*^{V600} mutations.

Results

BRAF^{V600E} mutations were detected in ECD biopsies from all 3 patients, and in samples of LCH epidermal infiltration from

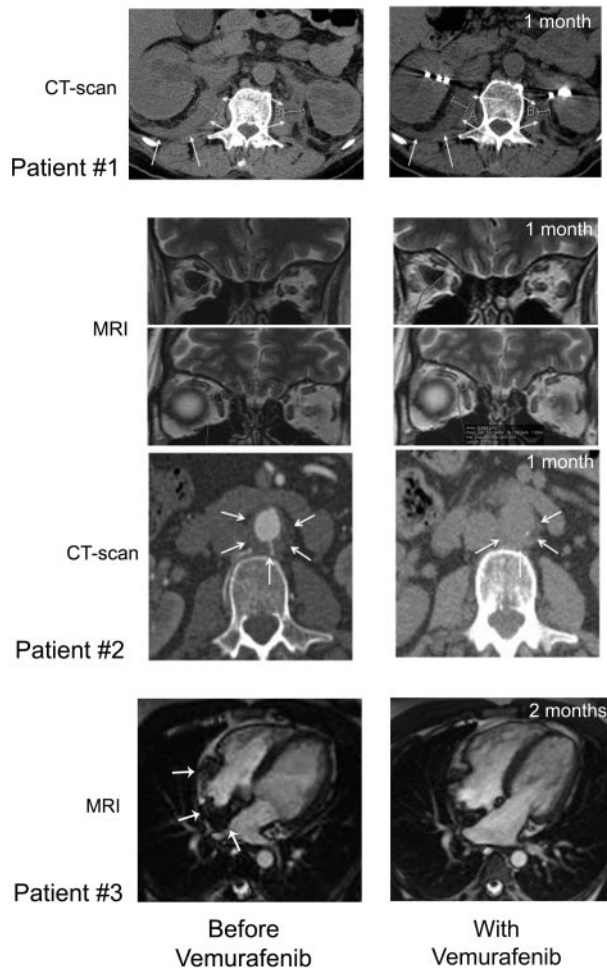


Figure 3. CT scan and MRI imaging assessment. Patient no. 1: Comparison of abdominal axial CT scans performed before (January 28, 2012; left) and on day 37 (May 23, 2012; right) of treatment showing regression of the infiltration around both kidneys (white arrows), evidenced by the decreased thickness (right kidney: 24.8 to 18.2 mm, left kidney 22 to 12.4 mm). Patient no. 2: Comparison of MRI performed before (left) and on day 36 (right) of vemurafenib treatment showing regression of ECD orbital infiltration. Comparison of abdominal axial CT scans performed before (March 29, 2012; left) and on day 39 (May 25, 2012; right) of vemurafenib treatment showing regression of the infiltration around abdominal aorta (white arrows): latero-aortic infiltration from 10.8 to 6.5 mm thick, and posterior infiltration from 6.5 to 4.6 mm thick. Patient no. 3: comparison of cardiac MRI, 4-chamber view: (A) February 21, 2012; see the infiltration of the atrial septum, the posterior wall and the free wall of the right atrium (white arrows); (B) July 19, 2012; note the regression of the infiltration.

patient no. 2. The expression of the V600E mutant BRAF protein in histiocytes from both ECD and LCH lesions was confirmed by immunohistochemistry (Figure 2).

The efficacy of vemurafenib

These 3 cases of refractory ECD with life-threatening manifestations associated with the *BRAF*^{V600E} mutation were all treated with vemurafenib. All patients provided consent for vemurafenib treatment after appropriate counseling.

Vemurafenib (initially given at 1920 mg/d) was tapered in all 3 patients to 960 mg/d (on days 30, 30, and 20, respectively) due to cutaneous side effects and was maintained until further follow-up. 2 These side effects were classified as grade 2 according to the Common Terminology Criteria for Adverse Effects (CTAE). No other toxicities or adverse events were observed. All patients

showed clear clinical improvement within a few days of initiation of this treatment.

Patient no. 1. Vemurafenib was started at 1920 mg/d (b.i.d.) on April 19, 2012 and was tapered to 960 mg/d from day 30 due to erythema, and was thereafter maintained at this dose. Within a few days of the initiation of treatment, itching disappeared. Evaluation on day 30 showed an improvement of creatinine (190 to 161 μ M), GGT (936 to 300 U/l) and alkaline phosphatase (644 to 177 U/l) values. On day 62, GGT was 183 U/l, PAL 146 U/l, and creatinine 170 μ M. CRP was normalized by day 30 (Figure 4), and remained under 5 mg/L on day 62. PET was performed after 30 days of vemurafenib treatment and the findings compared with those obtained 4 months earlier: there was a substantial improvement of all lesions (Figure 1), with a mean Standardized Uptake Value (SUV) change of -70% (range, -66% to -80%); the change within soft tissue and bone was similarly -70% (range, -51% to -78% ; supplemental data, available on the *Blood* Web site; see the Supplemental Materials link at the top of the online article). Thoraco-abdominal CT after 37 days of treatment showed a significant reduction of periaortic infiltration (Figure 3). This cannot be attributed to PEG-IFN treatment, withdrawn on March 31, 2012, because several

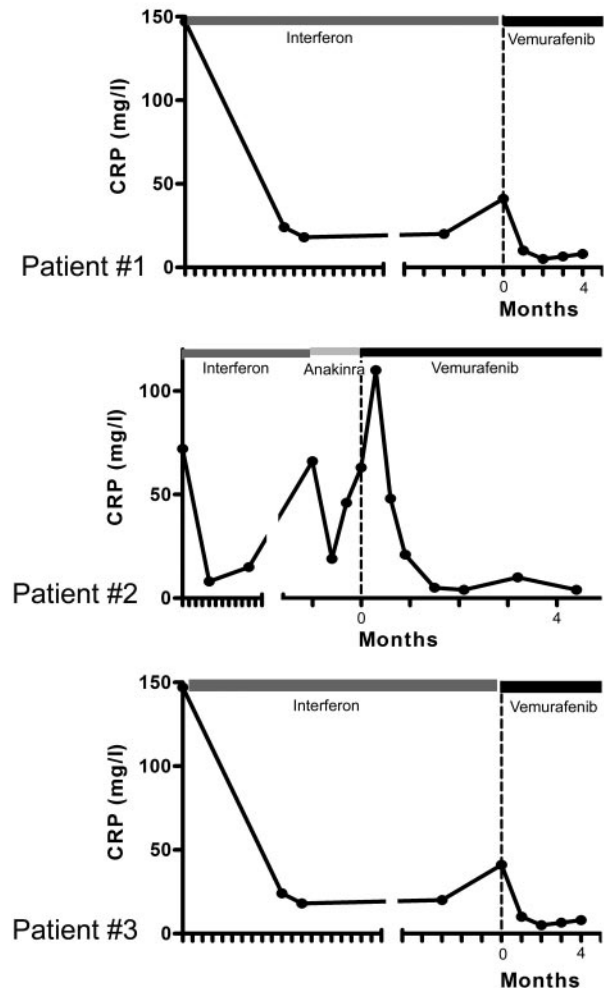


Figure 4. Evolution of CRP levels under treatment. Patient no. 1: Blood CRP concentrations, correlating with initial response and secondary resistance to PEG-IFN treatment, and returning to normal values (< 5 mg/L) under vemurafenib. Patient no. 2: an initial CRP increase was associated with headaches and fever (39°C); CRP concentrations returned to normal values after 1 month of treatment. Patient no. 3: CRP concentrations returned to normal values after one month of treatment. Time 0 corresponds to initiation of vemurafenib treatment, and each graduation corresponds to 1 month.

other markers clearly indicated that the patient was a nonresponder (high CRP values, hydronephrosis and pyelocaliceal dilation, worsening of PET findings). Hydronephrosis and pyelocaliceal dilation resolved completely. Note that the PET assessment at 4 months showed that the decrease of FDG uptake had been sustained: uptake was lower than that observed after the first month (Figure 1). Aortic MRI after 4 months disclosed a marked regression of peri-aortic sheathing relative to that observed by CT-scan in May 2012. The CRP value remained low on day 123 of treatment (Figure 4).

Patient no. 2. Vemurafenib was administered at 1920 mg/d (b.i.d) from April 17 with a transient interruption of 2 days (days 12 to 14) due to headaches and fever at 39°C. The CRP value increased to 114 mg/L (May 1); lumbar puncture was normal, blood cultures were negative, and both physical examination and thoracic CT-scan ruled out pneumopathy. The clinical symptoms rapidly disappeared and CRP values declined (100 and 48 mg/L on May 2 and 3). We were able to resume treatment at full dose at day 14. Our impression was that this transient episode was perhaps a viral infection, or cytokine-related, but not due to the disease or vemurafenib treatment. The dose was tapered to 960 mg/d from day 30 due to itching, skin rash and keratosis pilaris lesions which had appeared a few days before. Itching was not attributed to LCH involvement but appeared to be a consequence of the cutaneous toxicity of vemurafenib. Skin manifestations disappeared within days of the reduction of the dose which was maintained at 960 mg/d until further follow-up.

After a few days, histiocytic skin lesions resolved (Figure 2), and the pain in the right eye disappeared such that morphine could be stopped. A new skin biopsy confirmed the absence of histiocytic infiltration of the epidermis and hypodermis. CRP was normalized by day 30 (Figure 4), and was 5.2 mg/L ($N < 5$) on day 48. PET 31 days after initiation of vemurafenib was compared with that performed 2 months earlier: the change in the mean SUV was -57% (range, -51% to -67%) and that in soft tissue and bone was -70% (range, -56% to -78% ; Figure 1 and supplemental data). Orbit MRI on day 36 showed a 26% to 66% decrease of the retro-orbital infiltration (Figure 3 and supplemental data). Thoraco-abdominal CT on day 39 demonstrated a 30% to 40% decrease of the posterior and lateral peri-aortic infiltration (Figure 3), and the absence of the previously observed interlobular septa thickening, characteristic of pulmonary involvement of ECD. The CRP value remained below 5 mg/L on day 141 of treatment (Figure 4), and the patient was asymptomatic, with the absence of orbital pain.

Patient no. 3. Vemurafenib was administered at 1920 mg/d (b.i.d) from May 9 to May 29: the dose was tapered to 960 mg/d (b.i.d) due to pilar keratosis and erythema. One month later, the CRP level was 10 mg/L, the thickness of xanthelasmas had diminished, and PET displayed significantly decreased uptake in the basilar region and by the long bones. In July 2012, the CRP value was normal. The most striking feature was the significant improvement of the cardiac MRI on July 19: right atrial wall infiltration had regressed substantially (Figure 3). On day 119 of treatment, the CRP value was still low, at 8 mg/L (Figure 4).

Discussion

This is the first report of the use of vemurafenib in ECD patients carrying the *BRAF*^{V600E} mutation, with a multisystemic form of the disease refractory to IFN. The treatment was extremely and rapidly effective in all 3 patients: clinical symptoms improved, CRP values normalized, all pathologic uptakes on PET regressed substantially, peri-vascular sheathing regressed, and heart infiltration improved

markedly; the LCH skin lesions of patient no. 2 disappeared and the severity of the orbital lesion decreased.

PET assessment of treatment of cases of ECD has not previously documented such rapid efficacy. IFN treatment has a much more subtle and slow effect on the regression of uptakes.¹³ For patient no. 1, there was a mean regression of 70% of visceral and bone ¹⁸F-fluorodeoxyglucose uptakes at month 1, and the therapeutic response observed at month 4 was even better. Substantial regression of peri-vascular sheathing and disappearance of hydronephrosis (CT), as well as normalization of measures of CRP and liver enzymes confirmed the excellent therapeutic efficacy. The benefits of treatment were similar in patient no. 2, with 57% to 70% regression of visceral and bone ¹⁸F-fluorodeoxyglucose uptakes, regression of peri-aortic and orbital infiltrations, and normalization of CRP values.

Imaging and analysis of biologic markers demonstrated tumor regression within 40 days in patients 1 and 2, and for patient no. 3 there was a major regression of heart infiltration by day 71. Moreover, the clinical benefits, with the resolution of pruritus for patient no. 1 and of skin lesions and orbital pain for patient no. 2, were apparent within a few days. The Pitié-Salpêtrière Hospital has cared for 84 ECD patients between 1991 and 2012, and there have been no previous cases of such remarkable and rapid clinical, biologic, and imaging improvements.

Typical LCH infiltration has been reported in some patients with confirmed ECD. In patient no. 2, the *BRAF*^{V600E} mutation was detected in both types of histiocytes. LCH skin lesions disappeared rapidly under vemurafenib and this was confirmed by biopsy, suggesting that LCH patients may also benefit from vemurafenib treatment; the value of such treatment should be assessed in patients with pure LCH disease.

Contrasting with other types of histiocytosis, *BRAF*^{V600E} mutations are present in approximately half of the patients with ECD or LCH.⁶⁻⁸ Among the 84 ECD patients followed in our center, 17 (20.2%) have died of disease. Although an appropriate dosing schedule and treatment duration remain to be determined in clinical trials, our findings provide compelling evidence of the fast efficacy of BRAF inhibition in *BRAF*^{V600E}-associated ECD. The long-term efficacy of BRAF inhibition in ECD should also be studied, as secondary resistance develops in almost all cases of *BRAF*^{V600E}-associated melanoma.¹⁴ Patient no. 1 was asymptomatic at 4 months and had normal CRP values. At that time, follow-up PET assessment only revealed persistent bone uptake, which we believe should rather be interpreted as being a typical hallmark of the disease than a marker of disease activity. Nevertheless, the durability of the therapeutic response to vemurafenib remains unknown and should be evaluated over longer periods.

In view of the remarkable efficacy in the 3 cases we report, we believe that BRAF inhibition should be considered in a larger cohort of *BRAF*^{V600E}-associated histiocytosis patients, particularly those with life-threatening disease.

Acknowledgments

The authors thank Prof A. von Deimling (Heidelberg, Germany) for providing the anti-*BRAF*^{V600E} mouse monoclonal antibody VE1.

This work was supported in part by grants from the nonprofit organism Association pour la Recherche en Pathologie (AREP).

Authorship

Contribution: J.H., F.C.-A., J.-F.E., L.A., and Z.A. designed the research; J.H., F.C.-A., J.-F.E., L.A., P.M., F.C., P.C., A.D., and Z.A. collected the data; J.H., F.C.-A., J.-F.E., L.A., P.M., F.C., P.C., A.D., B.H., N.B., S.B., J.D., and Z.A. analyzed and interpreted the data; J.H., F.C.-A., J.-F.E., L.A., P.M., F.C., P.C., A.D., B.H., N.B., S.B., J.D., and Z.A. wrote the manuscript; and all authors approved the final manuscript.

Conflict-of-interest disclosure: J.H. received honoraria from Glaxo Smith Kline for counseling of patients with histiocytosis on the treatments with targeted therapies. J.-F.E. received honoraria from Roche and Glaxo Smith Kline for counseling patients with melanomas on the diagnosis and/or treatment with BRAF inhibitors. The remaining authors declare no competing financial interests.

Correspondence: Dr Julien Haroche, MD, PhD, Service de Médecine Interne 2, Groupe Hospitalier Pitié-Salpêtrière, 47-83 bd de l'Hôpital, 75013, Paris, France; e-mail: julien.haroche@psl.aphp.fr.

References

1. Haroche J, Arnaud L, Amoura Z. Erdheim-Chester disease. *Curr Opin Rheumatol*. 2012; 24(1):53-59.
2. Arnaud L, Hervier B, Néel A, et al. CNS involvement and treatment with interferon- α are independent prognostic factors in Erdheim-Chester disease: a multicenter survival analysis of 53 patients. *Blood*. 2011;117(10):2778-82.
3. Marchal A, Cuny JF, Montagne K, et al. Associated Langerhans cell histiocytosis and Erdheim-Chester disease. *Ann Dermatol Venereol*. 2011; 138(11):743-7.
4. Emile JF, Wechsler J, Brousse N, et al. Langerhans' cell histiocytosis. Definitive diagnosis with the use of monoclonal antibody O10 on routinely paraffin-embedded samples. *Am J Surg Pathol*. 1995;19(6):636-41.
5. Badalian-Very G, Vergilio JA, Degar BA, et al. Recurrent BRAF mutations in Langerhans cell histiocytosis. *Blood*. 2010;116(11):1919-23.
6. Satoh T, Smith A, Sarde A, et al. B-RAF Mutant Alleles Associated with Langerhans Cell Histiocytosis, a Granulomatous Pediatric Disease. *PLoS One*. 2012;7(4):e33891.
7. Sahn F, Capper D, Preusser M, et al. BRAFV600E mutant protein is expressed in cells of variable maturation in Langerhans cell histiocytosis. *Blood*. 2012;120(12):e28-34.
8. Haroche J, Charlotte F, Arnaud L, et al. High prevalence of *BRAF V600E* mutations in Erdheim-Chester disease but not in other non-Langerhans cell histiocytoses. *Blood*. 2012; 120(13):2700-3.
9. Chapman PB, Hauschild A, Robert C, et al. Improved survival with vemurafenib in melanoma with BRAF V600E mutation. *N Engl J Med*. 2011; 364(26):2507-16.
10. Dietrich S, Glimm H, Andrulis M, et al. BRAF Inhibition in Refractory Hairy-Cell Leukemia. *N Engl J Med*. 2012;366:2038-40.
11. Capper D, Preusser M, Habel A, et al. Assessment of BRAF V600E mutation status by immunohistochemistry with a mutation-specific monoclonal antibody. *Acta Neuropathol*. 2011;122(1): 11-19.
12. Moreau S, Saiag P, Aegerter P, et al. Prognostic value of *BRAF*^{V600} mutations in melanoma patients after resection of metastatic lymph nodes. *Ann Surg Oncol*. doi:2012;19(13):4314-4321.
13. Arnaud L, Malek Z, Archambaud F, et al. 18 F-Fluorodeoxyglucose-Positron Emission Tomography scanning is more useful in followup than in the initial assessment of patients with Erdheim-Chester disease. *Arthritis Rheum*. 2009;60(10): 3128-38.
14. Aplin AE, Kaplan FM, Shao Y. Mechanisms of resistance to RAF inhibitors in melanoma. *J Invest Dermatol*. 2011;131(9):1817-20.